New $Ba_5M_{5-x}Pt_xClO_{13}$ (M = Fe, Co) oxychlorides with layered perovskite-related structure

Nathalie Tancret, Pascal Roussel,* and Francis Abraham

Laboratoire de Cristallochimie et Physicochimie du Solide, UMR CNRS 8012, Ecole Nationale Supérieure de Chimie de Lille – Université des Sciences et Technique de Lille, BP 108, Av Mendeleiev, 59652 Villeneuve d'Ascq, Cedex, France

Abstract

Crystals of $Ba_5Fe_{5-x}Pt_xClO_{13}$ and $Ba_5Co_{5-y}Pt_yClO_{13}$ were prepared for x = 1.31, 1.51, 1.57, 1.59 and y = 0, 0.97 and 1.08 in a $BaCl_2$ flux and investigated by X-ray diffraction methods. These compounds adopt a 10H perovskite structure built from the stacking of BaO_3 and $BaOCl$ layers in the sequence $(BaO_3)_4(BaOCl)$ with space group $P6_3/mmc$. The cation sites within the trimeric unit of face-sharing octahedra are occupied by Co or Fe and Pt ions, while the tetrahedral sites formed between BaO_3 and $BaOCl$ layers are only occupied by Fe or Co. Moreover, oxygen stoichiometry indicates an average oxidation state for Co and Fe higher than +III, indicating the stabilization of Co^{4+} and Fe^{4+}.

© 2003 Elsevier Inc. All rights reserved.

Keywords: Oxychloride; X-ray diffraction; Crystal structure; Hexagonal perovskite

1. Introduction

Many compounds with hexagonal perovskite-type structure have been reported during the last years. These structures are characterized by the stacking of AO_3 (A = Ba, Sr, Ca) layers or by the alternation of AO_3 and "deficient" layers such as AX or AX_2 (X = O, Cl, Br); the largest family is obtained for A = Ba (for a review, see Ref. [1]). The main interest of this family of compounds is that they present a wide variety of interesting physical properties due to their particular crystallographic arrangement (electrical, magnetic, dielectric, optical and catalytic properties). Among them, the $Ba_5M_5ClO_{13}$ compounds (where M represents one, two or three metal atoms) were studied by several authors. The particularity of these compounds is the presence of a $BaOCl$ layer sandwiched between metal-containing slabs, the M atoms being located in octahedral and tetrahedral sites. Until now, three compounds have been reported: $Ba_5Co_5ClO_{13}$ [2], $Ba_5Fe_4PtClO_{12.5}$ [3] and $Ba_5In_2IrAl_2ClO_{13}$ [4] with respectively one, two and three kinds of metal. The particularity of the second compound ($Ba_5Fe_4PtClO_{12.5}$) being an apparent defi-

ciency in oxygen that gives only Fe(III). In $Ba_5Co_5ClO_{13}$, a small mistake led the authors to propose an erroneous charge disordered site preference model for the Co(III) and Co(IV) in tetrahedral and octahedral sites [2]. In fact, these compounds can be formulated $Ba_5(M1)_2(M2)_2M3ClO_{13-x}$, where $M1$ and $M3$ are in octahedral sites and $M2$ in a tetrahedral one. Attempts to synthesize other phases belonging to this family allowed us to bring out the existence of $Ba_5Fe_{5-x}Pt_xClO_{13}$ ($1.307 \leqslant x \leqslant 1.589$) solid solutions. For $Ba_5Co_{5-y}Pt_yClO_{13}$, in addition to the compound $Ba_5Co_5ClO_{13}$ (y = 0), a small domain around y = 1 is observed ($0.972 \leqslant y \leqslant 1.084$).

In this paper, syntheses and structural studies of both solid solutions are reported and comparison with the other compounds previously reported are made. Charge distribution (CD) calculations are also reported to state the repartition of metals in octahedral and tetrahedral sites and to prove the stabilization of Co(IV) and Fe(IV).

2. Experimental

2.1. Preparation and crystal growth

Several single-crystal samples of the $Ba_5Fe_{5-x}Pt_x$ ClO_{13} ($1.307 \leqslant x \leqslant 1.589$) and $Ba_5Co_{5-y}Pt_yClO_{13}$

---

*Corresponding author. Fax: +33-3-20-43-68-14.

E-mail addresses: pascal.roussel@ensc-lille.fr (P. Roussel), francis.abraham@ensc-lille.fr (F. Abraham).

($0 \leqslant y \leqslant 1.084$) solid solutions were prepared by a flux method. A 2 g mixture of $BaCO_3$ (Fisher, 99%), Fe_2O_3 (Johnson Matthey, high purity) or Co_3O_4 (Fluka, Assay > 71% (KT) Co) and $BaCl_2$, $2H_2O$ (Prolabo Rectapur) with the 2:1:4 or 2:2/3:4 ratio (preparation Nos. 2 and 6 in Table 1) was well ground in an agate mortar and heated in air at 1100°C for 48 h in a pure platinum crucible (99.9%). The products were then slowly cooled to 850°C at 0.5°C/min and finally quenched to room temperature. The excess of $BaCl_2$ was dissolved with hot water and black plates were extracted from the preparation.

Energy dispersive spectroscopy realized on several crystals revealed the presence of Pt in both phases, coming from the platinum crucible, in addition with Ba, Fe or Co, Cl and O elements. Measurements were performed using a JEOL JSM-5300 scanning microscope equipped with an IMIX system of Princeton Gamma Technology, at 15 kV. In order to try to control the platinum content, other synthesis were realized including powder Pt metal in the initial mixtures, in Pt crucible on the one hand and, in alumina crucible, on the other hand. Essentially, experiments in platinum crucible lead to expected compounds (Preparations 3 and 7 in Table 1); in alumina crucible, only one limit composition belonging to this family, without platinum, was obtained: $Ba_5Co_5ClO_{13}$ (Preparation 1, already previously reported [2]). Other syntheses did not lead to crystallized compounds, or other kinds of phases were obtained. They will be the subject of future studies. For the iron compounds, other reactions were attempted with iron oxalate FeC_2O_4, $2H_2O$ (Alpha Aesar, Johnson Matthey, 99.999%) as precursor instead of Fe_2O_3, with same conditions of preparation. Compounds with weak variations in the Fe/Pt ratio were obtained (Preparations 4 and 5 in Table 1). All the experiments allowed to prove the existence of solid solutions with Fe and Co: $Ba_5Fe_{5-x}Pt_xClO_{13}$ and $Ba_5Co_{5-y}Pt_yClO_{13}$, respectively, but with no control of x and y values during the synthesis due to the reaction of the platinum crucible. Finally, four Fe and three Co compositions could be obtained depending on several criteria: the Fe precursor

used, the presence or not of platinum powder in the initial mixture, and the nature of the crucible used for reaction (platinum or alumina). Results are gathered in Table 1. One can see that the adding of powder platinum in the initial mixture leads to a higher Pt/Fe or Pt/Co ratio for the same Fe or Co reactant. On the other hand, for the iron compounds, the use of iron oxalate leads to phases with higher iron content than with iron oxide. This can be attributed to a better reactivity of the oxalate in comparison with the oxide. Indeed, it is well known that the thermal decomposition of the oxalate precursor leads to an oxide with small grain size and high reactivity. The compound obtained in alumina crucible (Preparation 1 in Table 1) is quite surprising considering the initial mixture, the platinum powder initially introduced astonishingly does not appear in the final crystals.

2.2. Crystal structure determination

Numerous black plate-like crystals of $Ba_5(Co/Fe;Pt)_5ClO_{13}$, with dimensions given in Table 2, were used for X-ray crystallographic analysis. The X-ray intensity data were measured at room temperature on a Bruker SMART 1000 CCD-based X-ray diffractometer system equipped with a fine-focus Mo-target X-ray tube ($\lambda = 0.71073$ Å) operated at 2000 W power. The detector was placed at a distance of 5.41 cm from the crystal. A total of 1800 frames were collected with a scan width of 0.3° in ω and an exposure time of 20 s/frame covering the full sphere. The total data collection time was 13.5 h. The frames were integrated with the Bruker SAINT 6.22 software package [5] using a narrow-frame integration algorithm. The integration of the data using a hexagonal unit cell yielded a total of reflections from 4803 to 7189 (depending on the crystal type, see Table 2), to a maximum 2θ angle comprised between 58.1° and 63.02° (average redundancy 12.71). The final cell constants are based upon the refinement of the XYZ-centroids of all the reflections above $20\sigma(I)$. Analysis of the data showed no decay during data collection. Data were

Table 1
Obtained compounds vs. initial mixtures

Reactants	Ratio	Crucible	Single crystal obtained	No. prep.
$BaCO_3$–Co_3O_4–$BaCl_2$, $2H_2O$–Pt	4–4/3–8–1	Al_2O_3	$Ba_5Co_5ClO_{13}$	1
$BaCO_3$–Co_3O_4–$BaCl_2$, $2H_2O$	4–4/3–8	Pt	$Ba_5Co_{4.028}Pt_{0.972}ClO_{13}$	2
$BaCO_3$–Co_3O_4–$BaCl_2$, $2H_2O$–Pt	4–4/3–8–1	Pt	$Ba_5Co_{3.916}Pt_{1.0846}ClO_{13}$	3
$BaCO_3$–FeC_2O_4, $2H_2O$–$BaCl_2$, $2H_2O$	5–4–8	Pt	$Ba_5Fe_{3.693}Pt_{1.307}ClO_{13}$	4
$BaCO_3$–FeC_2O_4, $2H_2O$–$BaCl_2$, $2H_2O$–Pt	5–4–8–1	Pt	$Ba_5Fe_{3.488}Pt_{1.512}ClO_{13}$	5
$BaCO_3$–Fe_2O_3–$BaCl_2$, $2H_2O$	4–2–8	Pt	$Ba_5Fe_{3.435}Pt_{1.565}ClO_{13}$	6
$BaCO_3$–Fe_2O_3–$BaCl_2$, $2H_2O$–Pt	4–2–8–1	Pt	$Ba_5Fe_{3.411}Pt_{1.589}ClO_{13}$	7
$BaCO_3$–Fe_2O_3–$BaCl_2$, $2H_2O$–Pt	4–2–8–1	Al_2O_3	No single crystals	
$BaCO_3$–FeC_2O_4, $2H_2O$–$BaCl_2$, $2H_2O$–Pt	5–4–8–1	Al_2O_3	No single crystals	
$BaCO_3$–FeC_2O_4, $2H_2O$–$BaCl_2$, $2H_2O$	5–4–8	Al_2O_3	No single crystals	

Table 2
Crystal data for the single crystals compositions obtained from the structures refinement

Formula	$Ba_5Co_5ClO_{13}$	$Ba_5Co_{4.028}Pt_{0.972}ClO_{13}$	$Ba_5Co_{3.916}Pt_{1.084}ClO_{13}$	$Ba_5Fe_{3.693}Pt_{1.307}ClO_{13}$	$Ba_5Fe_{3.488}Pt_{1.512}ClO_{13}$	$Ba_5Fe_{3.435}Pt_{1.565}ClO_{13}$	$Ba_5Fe_{3.411}Pt_{1.589}ClO_{13}$
Prep no.	1	2	3	4	5	6	7
Crystallographic data							
Crystals dimensions	$90 \times 140 \times 25$	$140 \times 200 \times 25$	$120 \times 160 \times 25$	$140 \times 250 \times 25$	$130 \times 150 \times 25$	$50 \times 100 \times 25$	$130 \times 180 \times 25$
Formula weight (g/mol)	1224.8	1489.47	1519.97	1573.33	1630.42	1645.17	1651.86
Unit cell dimensions (Å)	$a = 5.6690(6)$	$a = 5.7055(6)$	$a = 5.7100(6)$	$a = 5.7986(6)$	$a = 5.7933(6)$	$a = 5.7795(6)$	$a = 5.7965(6)$
	$c = 24.304(3)$	$c = 24.736(3)$	$c = 24.809(3)$	$c = 25.0968(3)$	$c = 25.164(3)$	$c = 25.080(3)$	$c = 25.141(3)$
Cell volume ($Å^3$)	676.4	697.3	700.5	730.8	731.4	725.5	731.5
Density, calculated (g/cm^3)	6.011	7.091	7.204	7.148	7.401	7.529	7.497
Intensity collection							
θ range (deg.)	3.35–29.05	3.29–31.45	1.64–31.51	3.25–31.10	1.62–31.31	1.62–31.14	3.24–31.33
Data collected	$-7 \leqslant h \leqslant 7$	$-8 \leqslant h \leqslant 7$	$-8 \leqslant h \leqslant 8$	$-8 \leqslant h \leqslant 8$	$-7 \leqslant h \leqslant 8$	$-8 \leqslant h \leqslant 8$	$-8 \leqslant h \leqslant 8$
	$-7 \leqslant k \leqslant 7$	$-8 \leqslant k \leqslant 8$	$-7 \leqslant k \leqslant 8$	$-8 \leqslant k \leqslant 8$	$-8 \leqslant k \leqslant 8$	$-8 \leqslant k \leqslant 8$	$-8 \leqslant k \leqslant 8$
	$-31 \leqslant l \leqslant 32$	$-34 \leqslant l \leqslant 35$	$-36 \leqslant l \leqslant 35$	$-35 \leqslant l \leqslant 35$	$-36 \leqslant l \leqslant 34$	$-34 \leqslant l \leqslant 36$	$-36 \leqslant l \leqslant 36$
No. of reflections measured	4803	5897	6717	6546	7189	6631	6110
No. of independent reflections	398	499	495	508	521	507	520
Redundancy	12.07	11.82	13.57	12.89	13.80	13.08	11.75
No. of unique reflections ($I > 3\sigma(I)$)	290	393	398	426	436	382	383
μ_l(Mo, $K\alpha$)	20.52	37.07	38.87	40.68	44.16	45.43	45.47
T_{max}/T_{min}	0.4913	0.5494	0.4934	0.1955	0.4558	0.5935	0.3127
$R(F^2)_{int}$ (before absorption correction)	13.0	35.9	22.9	28.2	20.7	12.1	30.7
$R(F^2)_{int}$ (after absorption correction)	4.88	3.72	5.18	4.62	4.73	5.16	4.59
Refinement							
No. of parameters	27	29	29	29	29	29	29
$R(F)$ obs/all	2.38/4.92	2.41/3.86	2.25/3.52	2.62/3.70	2.62/3.53	4.17/7.04	2.55/4.89
$wR(F)$ obs/all	1.94/2.02	2.39/2.42	2.28/2.34	2.86/2.90	2.68/2.71	3.42/3.48	2.18/2.25
GOF all/obs	1.88/2.14	2.59/2.90	2.00/2.19	2.72/2.96	2.59/2.81	3.36/3.85	2.06/2.36
Isotropic secondary extinction[a]	0.0268(16)	0.021(2)	0.037(3)	0.043(3)	0.072(4)	0.011(2)	0.0082(12)
Max, min $\Delta\rho$ ($e^-/Å^3$)	5.08/−5.15	3.47/−3.13	2.43/−2.63	3.07/−3.20	2.41/−3.93	6.89/−8.14	5.03/−4.17
Distances residual peaks—atoms (Å)	Max–Ba2: 0.70	Max–Cl: 0.97	Max–Ba2: 1.46	Max–Ba2: 1.23	Max–O3: 0.73	Max–Ba2: 0.21	Max–Ba2: 0.37
	Min–O3: 1.37	Min–O2: 1.40	Min–Co2: 0.49	Min–Ba3: 1.31	Min–Fe1: 1.13	Min–Ba3: 1.38	Min–Cl: 0.47

[a] Becker and Coppens type I, Gaussian distribution [8].

corrected for absorption effects using a semi-empirical method (SADABS 2.03—Bruker/Siemens Area Detector Absorption and other corrections [6]) with ratio minimum, maximum transmission coefficients given Table 2.

The structure was refined using the JANA2000 Software Package [7], using the hexagonal space group $P6_3/mmc$, with $Z = 2$ for the formula unit $Ba_5(Co/Fe, Pt)_5ClO_{13}$. The final anisotropic full-matrix least-squares refinement on F converged at R values given in Table 2.

3. Results and discussion

3.1. Description of the structure

The atomic coordinates and isotropic atomic displacement parameters obtained for the seven structures are listed in Table 3. In Fig. 1, a view of the structure, in projection along [010], is given. This structure can be described in two different ways. In the first one, it can be viewed as a network of polyhedra. Indeed, two kinds of polyhedra can be observed: $M1O_6$ and $M3O_6$ octahedra and $M2O_4$ tetrahedra. Octahedra are linked together through faces to form $(M1)_2M3O_{12}$ units, and tetrahedra are linked together by a corner to form $(M2)_2O_7$ units. The structure is then built by the alternation of these two kinds of units along the [001] direction: a $(M1)_2M3O_{12}$ face-shared octahedra trimeric unit is sandwiched by a $(M2)_2O_7$ corner-shared tetrahedra unit and so on. Ba^{2+} cations are then located into the cavities formed by the oxygen and chlorine anions. They are distributed onto three crystallographic sites. The first one (Ba3) occupies a large cage formed by 12 oxygen atoms (Fig. 2a) with Ba–O distances ranging 2.91–3.30 Å. The second type of barium (Ba2) is coordinated by nine oxygen atoms and one chlorine atom. Ba–O distances are comprised between 2.65 and 2.95 Å and the Ba–Cl one is 3.05 Å. The environment of Ba2 is related to the environment of Ba3 just in replacing three oxygen atoms by one chlorine atom (Fig. 2a). In the same manner, the surrounding of the last type of barium (Ba1) can be deduced from that of Ba3 just by replacing three oxygen atoms of the "equatorial" plane by three chlorine atoms (Fig. 2b). Ba–O distances range 2.97–3.35 Å while the three Ba–Cl distances are equal to 3.35 Å. Note that the conformation of the surrounding of both Ba3 and Ba2 is very similar. Indeed, the six "equatorial" oxygen atoms and the three "apical" ones are in the same orientation for Ba2 and Ba3 (Fig. 2c). This is not the case for Ba1, the quasi-hexagon formed by three O and three Cl atoms (in bold, Fig. 2d) is rotated of 30° in relation to the Ba3 surrounding. To sum up, the Ba1 environment can be deduced from the Ba3 environment, just in replacing three oxygen out of six by three chloride, and also in rotating the resulting

plane of 30°, while the Ba2 surrounding is deduced by replacing three "apical" oxygen atoms by one chlorine. Finally, the chlorine atom is surrounded by five barium atoms forming a trigonal bipyramid with distances ranging 2.95–3.27 Å (Fig. 3).

The second method of describing this structure type is based on the stacking of compact hexagonal [BaX] layers (X=O$_3$ or O–Cl), where metallic cations are located into the octahedral or tetrahedral sites formed by this pile. Indeed, this structure can be viewed as the stacking along the [001] direction of 10 layers (Fig. 1), $([BaO_3]_4[BaOCl])_2$. This compound, hexagonal and constructed by the stacking of 10 compact layers, is thus deriving from the 10H polytype [1]. Another way to describe this type of structure, firstly introduced by Katz and Ward [9], is to consider a stacking of "cubic" and "hexagonal" layers: a letter "c" is used to designate a "cubic", i.e., a layer for which the two neighboring layers are of different types; a letter "h" stands for a "hexagonal" layer, i.e., a layer sandwiched by two layers of the same type. Using this terminology, $Ba_5(Co/Fe;Pt)_5ClO_{13}$ is then described by the sequence (hch'ch)$_2$.

3.2. Characterization of the new solid solution and metal repartition

The previously reported magnetism study of $Ba_5Co_5ClO_{13}$ revealed the presence of Co^{4+} in this compound [2]. However, in this study, the authors concluded to the impossibility of a hypothetical composition with a charge-ordered site preference model for the cobalt ions. They concluded to a mixed octahedral and tetrahedral Co^{3+}/Co^{4+} (Table 4). During our study, we have re-examined this hypothesis and we can conclude that there was a small misinterpretation in this paper. Indeed, if one consider that Co^{3+} is located exclusively in octahedral $M1$ and $M3$ sites (see Table 3), while Co^{4+} is located in tetrahedral $M2$ sites, we can propose the formula $Ba_5Co_3^{3+}Co_2^{4+}ClO_{13}$ to explain a completely charge-ordered model. This formula is in perfect agreement with the proposed oxygen stoichiometry. However, the goal of the present paper is not to deal with either a completely charge-ordered model or with a mixed one, but the interesting result of the study is that, in $Ba_5Co_5ClO_{13}$, it is clear that Co ions with a +4 valence are observed. The platinum substituted compound leads to exactly the same crystallographic structure, so the presence of Co^{4+} is no doubtful in the solid solution $Ba_5Co_{5-y}Pt_yClO_{13}$. The framework being exactly the same one with the iron substituted structures, the analogy with cobalt phases involves the presence of Fe^{4+}. Unfortunately, this existence could not be proved by physical analysis. Indeed, Leib et al. [3] did not see Fe^{4+} by Mossbauer method, so in the chemical formula proposed, $Ba_{10}Fe_8Pt_2Cl_2O_{25}$, supposing all Fe in (+III)

Table 3
Atomic coordinates and isotropic displacement parameters (in Å^2)

Prep. no.	Atom symbol	Wyck. symbol	Occ.	x	y	z	U_{iso} (Å^2)
1	Ba1	2b	1	0	0	1/4	0.0156(3)
2							0.0175(3)
3							0.0172(3)
4							0.0205(3)
5							0.0204(3)
6							0.0247(6)
7							0.0257(3)
1	Ba2	4f	1	1/3	2/3	0.37135(3)	0.0098(2)
2						0.37017(3)	0.0108(2)
3						0.36998(3)	0.0095(2)
4						0.37178(3)	0.0099(2)
5						0.37153(3)	0.0095(2)
6						0.37068(5)	0.0133(4)
7						0.37125(3)	0.0117(3)
1	Ba3	4f	1	1/3	2/3	0.95991(3)	0.0101(2)
2						0.95928(3)	0.0123(2)
3						0.95901(3)	0.0115(2)
4						0.96057(3)	0.0130(2)
5						0.96079(3)	0.0130(2)
6						0.96048(5)	0.0167(4)
7						0.96069(3)	0.0145(2)
1	Co1	4e	1	0	0	0.60285(6)	0.0077(4)
2	Co1/Pt1		0.756(3)/0.244			0.60476(4)	0.0095(3)
3	Co1/Pt1		0.784(3)/0.216			0.60534(4)	0.0085(3)
4	Fe1/Pt1		0.777(3)/0.223			0.60836(5)	0.0084(4)
5	Fe1/Pt1		0.704(3)/0.296			0.60821(4)	0.0078(3)
6	Fe1/Pt1		0.659(5)/0.341			0.60776(5)	0.0096(5)
7	Fe1/Pt1		0.683(3)/0.317			0.60760(3)	0.0099(3)
1	Co2	4f	1	1/3	2/3	0.82316(6)	0.0093(5)
2						0.82160(6)	0.0110(4)
3						0.82155(5)	0.0100(4)
4	Fe2	4f	1	1/3	2/3	0.82110(7)	0.0081(5)
5						0.82097(6)	0.0074(4)
6						0.81850(12)	0.0113(8)
7						0.82051(7)	0.0113(5)
1	Co3	2a	1	0	0	0	0.0059(5)
2	Pt3/Co3		0.484(4)/0.516				0.0080(3)
3	Pt3/Co3		0.652(4)/0.348				0.0071(2)
4	Pt3/Fe3		0.861(5)/0.139				0.0065(2)
5	Pt3/Fe3		0.920(4)/0.080				0.0063(2)
6	Pt3/Fe3		0.907(7)/0.093				0.0070(3)
7	Pt3/Fe3		0.915(4)/0.085				0.0077(2)
1	Cl	2c	1	1/3	2/3	1/4	0.0267(15)
2							0.0268(13)
3							0.0277(12)
4							0.0365(2)
5							0.0373(2)
6							0.043(4)
7							0.0368(2)
1	O1	12k	1	0.3225(9)	0.1612(5)	0.35063(18)	0.0147(11)
2				0.3222(10)	0.1611(5)	0.34881(19)	0.0194(10)
3				0.3214(9)	0.1607(4)	0.34867(18)	0.0179(9)
4				0.3256(11)	0.1628(5)	0.3487(2)	0.0213(13)
5				0.3248(10)	0.1624(5)	0.3485(2)	0.0211(11)
6				0.3259(19)	0.163(1)	0.3483(3)	0.025(2)
7				0.3250(11)	0.1625(6)	0.3486(2)	0.0247(13)

Table 3 (*continued*)

Prep. no.	Atom symbol	Wyck. symbol	Occ.	x	y	z	U_{iso} (Å^2)
1	O2	12*k*	1	0.7062(8)	0.8531(4)	0.44984(18)	0.0079(9)
2				0.7001(9)	0.8500(4)	0.44822(18)	0.0121(9)
3				0.6985(8)	0.8492(4)	0.44747(16)	0.0115(8)
4				0.692(1)	0.8460(5)	0.4488(2)	0.0128(11)
5				0.6925(9)	0.8463(5)	0.44839(19)	0.0123(10)
6				0.6950(15)	0.8475(8)	0.4486(3)	0.0113(16)
7				0.6929(9)	0.8465(5)	0.44861(18)	0.0121(10)
1	O3	2*d*	1	1/3	2/3	3/4	0.049(4)
2							0.055(5)
3							0.054(4)
4							0.069(7)
5							0.068(6)
6							0.085(12)
7							0.056(5)
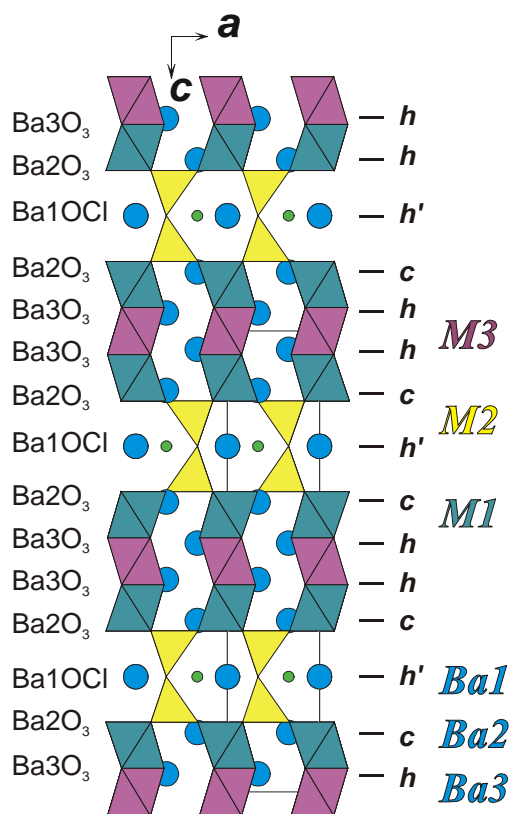
Fig. 1. Projection along [010] of the crystal structure of Ba$_5$(M, Pt)$_5$ClO$_{13}$, M = Fe, Co compounds showing the framework built from face and corner sharing of $(M,Pt)O_6$ octahedra and MO_4 tetrahedra. The BaO$_3$ and BaOCl stacking along [001] is shown on both sides of the polyhedron framework representation.

Fig. 2. The Ba coordination polyhedra and their relationships in Ba$_5$(M,Pt)$_5$ClO$_{13}$, M = Fe, Co compounds. Ba3 adopts the classical 12-coordination of metals in *hcp* structure, Ba2 is deduced by replacing an O$_3$ triangle by one Cl atom (a and c), Ba1 is obtained from Ba3 by replacing half the oxygen of the hexagon and by rotating the basal hexagon of 30° (b and d).

oxidation state, one oxygen atom is missing to obtain electrical neutrality in the molecule. In our compounds, XANES analyses were performed but the results did not all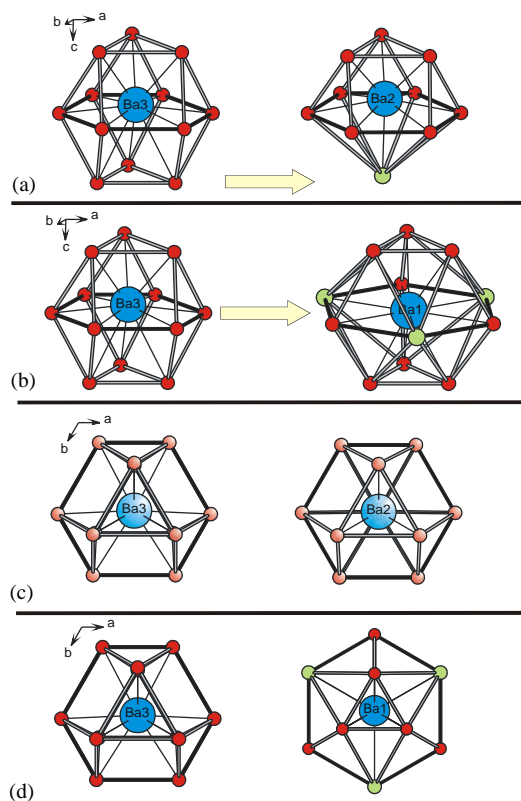ow to detect Fe^{4+} or Co^{4+}. But the hypothesis of one missing oxygen proposed by Leib et al. [3] is quite doubtful because a mixed occupation site Fe/Pt was supposed by the authors with an arbitrary 50/50 ratio and was further eliminated because of bad structural

results (R factor increased from 0.07 to 0.17). In the present study, we tried a different model. Firstly, we tried the model published by Leib et al. [3], i.e., the $4e$ octahedral sites (labeled $M1$) and the $4f$ tetrahedral sites ($M2$) fully occupied by iron, and the octahedral $M3$ site exclusively filled by platinum. At this level, the R value was $\approx 8\%$, the thermal parameter U of O3 was very strong ($U \approx 0.20\,\text{Å}^2$), and the U value of the Fe1 site was negative ($\approx -0.016\,\text{Å}^2$), indicating an excess of electronic density on this site. Moreover, a Fourier-difference series showed a large hole at the Pt position, indicating a lack of electrons on this site. We concluded that the $M1$ and $M3$ sites could be occupied either by iron and platinum. We then tried the other model proposed by Leib et al. [3] consisting of an arbitrary fixed 50/50 mixed Fe–Pt sites. The tetrahedral $M2$ site is only occupied by iron, since tetrahedral environment for Pt is unlikely. Results were as bad as those obtained by Leib et al. [3]: an increase of the R value, and still the same problems in the Fourier-difference series. We finally undertook to do a refinement with mixed Fe–Pt sites with, as only restraint, full "metal" site occupations, i.e., occ[Pt] + occ[Fe] = 1 for $M1$ and $M3$ sites. R rapidly dropped at values $\approx 3\%$ (depending on the preparation) and formula reported in Table 1. Moreover, all the previously observed problems disappeared, i.e., no negative or abnormally high values of thermal para-

meters were found, neither abnormal "big" holes or peaks in final Fourier-difference series. Distances between the Fourier-difference residual peaks and the positioned atoms are reported in Table 2. Note also that the oxygen atom sites were constrained to be fully occupied. After our study, we can conclude to a partial occupation of some sites by Fe or Co and Pt atoms but these ratios were refined to lead to the different formula reported in Table 1. This result confirms the hypothesis of O_{13} stoichiometry (O(3) fully occupied) and the presence of Fe^{4+} or Co^{4+} by analogy with $Ba_5Co_5ClO_{13}$ [2]. Moreover, crystallographic results are better than those proposed by Leib et al. [3]: R close to 0.03 instead of 0.07. The proportion of Fe^{4+} (or Co^{4+}) is very small compared to Fe^{3+} (or Co^{3+}); so it is not surprising that the different physical methods that we used did not allow us to detect it.

Another compound with the same structure has already been reported by Neubacher and Muller-Buschbaum [4], $Ba_5IrIn_2Al_2ClO_{13}$. It is also hexagonal, SG $P6_3/mmc$, $a = 5.860$ and $c = 25.101\,\text{Å}$, and in this compound, triple face-sharing octahedra units (arranged around Ir^{5+} and In^{3+}), are connected at the corners to Al_2O_7 double corner-sharing units. A charge-ordered model has been proposed for this compound: Ir^{5+} are located in the $2a$ $M3$ site, In^{3+} on $4e$ $M1$ site, and Al^{3+} on $4f$ tetrahedral $M2$ site (Table 4). The formula $Ba_5^{2+}Ir^{5+}In_2^{3+}Al_2^{3+}Cl^{1-}O_{13}^{2-}$, in good agreement with the oxygen stoichiometry, has thus been proposed. However, atomic displacement parameter for $M2$ site occupied by Al is particularly weak ($B = 0.008(126)\,\text{Å}^2$) so a statistical distribution of Al and In in $M2$ (and consequently on $M1$) cannot be ruled out.

This study shows the existence of new solid solutions $Ba_5M_{5-x}Pt_xClO_{13}$ (M = Fe, Co) with different domains: ($1.307 \leqslant x \leqslant 1.589$) for M = Fe and ($0.972 \leqslant x \leqslant 1.084$) for M = Co, in addition with the compound $Ba_5Co_5ClO_{13}$ ($x = 0$). However, the theoretical limits are the same and can be predicted. Indeed, two extreme models can be proposed: the first one, experimentally observed for Co compounds, consist of all the "metal" sites occupied by Fe or Co. It is the low limit of the solution solid ($x = 0$) with a formula $Ba_5(Fe/Co)_5ClO_{13}$. For the high limit, we just have to envisage all octahedral sites occupied by Pt and tetrahedral ones by Fe or Co. This hypothetical formula limit is then $Ba_5(Fe/Co)_2Pt_3ClO_{13}$ corresponding to $x = 3$. Thus the theoretical limit for these
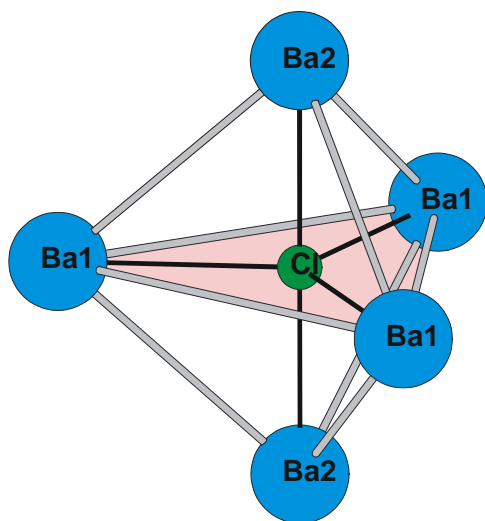

Fig. 3. The trigonal bipyramid coordination of Cl by Ba atoms in the $Ba_5(M,Pt)_5ClO_{13}$, M = Fe, Co compounds.

Table 4
Charge distribution in the $Ba_5M_{5-x}Pt_xClO_{13}$ (M = Fe, Co) compounds

	$Ba_5Co_5ClO_{13}$ (2)	$Ba_5In_2IrAl_2ClO_{13}$ (4)	$Ba_5Fe_4PtClO_{12.5}$ (3)	$Ba_5Fe_{5-x}Pt_xClO_{13}$ This work	$Ba_5Co_{5-x}Pt_xClO_{13}$ This work
$M2$	Co^{III}/Co^{IV}	Al^{III}	Fe^{III}	Fe^{III}/Fe^{IV}	Co^{III}/Co^{IV}
$M1$	Co^{III}/Co^{IV}	In^{III}	Fe^{III}	$Fe^{III}/Fe^{IV}/Pt^{IV}$	$Co^{III}/Co^{IV}/Pt^{IV}$
$M3$	Co^{III}/Co^{IV}	Ir^{IV}	Pt^{IV}	$Fe^{III}/Fe^{IV}/Pt^{IV}$	$Co^{III}/Co^{IV}/Pt^{IV}$

$Ba_5(Fe/Co)_{5-x}Pt_xClO_{13}$ solid solutions is $0 \leqslant x \leqslant 3$. Even if we succeeded to synthesize one limit of solid solution for Co ($Ba_5Co_5ClO_{13}$, compound 1), the other limits could not be obtained. This synthesis was realized in an alumina crucible because all preparations in platinum crucible lead to compounds containing this metal. Other syntheses effectuated into alumina crucibles did not allow to obtain single crystals belonging to this family of phases; either we did not obtain a correct compound or we synthesized other phases which will be further studied. In all preparations, we do not control the composition of the synthesized compound because there is a reaction with the crucible when the reaction is performed into platinum (preparations 2–7), $BaCl_2$, $2H_2O$ is added in excess so the quantity of barium cannot be known and, even if platinum is present in the original mixture, the final product does not necessarily contain platinum (preparation 1). The composition of synthesized compounds cannot be predicted for the reasons exposed above, so the theoretical limits of solid solutions cannot be easily reached experimentally.

3.3. Analysis of the valence state

CD analysis [10–12] has been performed on the (Fe,Pt) and (Co,Pt) compounds, and also on the non-substituted one. According to Nespolo et al. [11], the CD method, previously introduced as a development of the "classical" bond strength Pauling's definition [13] and of the bond valence (BV) approach [14], can provide important structural details. Different from BV, the CD description depends upon the geometry of each co-ordination polyhedron, in using the true bond distance in a self-consistent algorithm rather than exploiting empirical curves, as in the BV approach: the contribution of each bond distance is scaled to an empirical parameter (the so-called normalizing parameter) in the BV method, but to the shortest bond length in each polyhedron in the CD approach. Moreover, in the presence of cationic substitution, since the parameters used in the BV method depend upon the cation–anion pair, the computed valence is biased. On the other hand, if the geometry of the polyhedron does not change, since the CD method depends only upon the geometry of this coordination polyhedra, no difference is obtained by substituting cations with the same formal oxidation number. Finally, the ratio q/Q of the formal oxidation number to the calculated charge can be used to estimate the correctness of the structure (cation ratio) and to evaluate over or under bonding effects (anion ratio). A q/Q ratio close to 1 is expected for the cations when the structure is correctly solved; on the other hand, the q/Q ratio for the anions significantly differ from 1 when an over/under bonding effect is present. Note, in addition, that Hoppe et al. [10] showed that the CD method

Table 5
Charge distribution for the different compounds of Table 1

Formula	$Ba_5Co_5ClO_{13}$	$Ba_5Co_{4.028}Pt_{0.972}ClO_{13}$	$Ba_5Co_{3.916}Pt_{1.084}ClO_{13}$	$Ba_5Fe_{3.693}Pt_{1.307}ClO_{13}$	$Ba_5Fe_{3.488}Pt_{1.512}ClO_{13}$	$Ba_5Fe_{3.435}Pt_{1.565}ClO_{13}$	$Ba_5Fe_{3.411}Pt_{1.589}ClO_{13}$	$Ba_5Fe_4PtClO_{13}$
Prep no.	1	2	3	4	5	6	7	
Formal oxidation state of Co or Fe	3.40	3.26	3.23	3.19	3.14	3.13	3.12	3
Ba1	2/1.978/1.011	2/1.994/1.003	2/2.005/0.998	2/1.960/1.020	2/1.977/1.011	2/1.981/1.009	2/1.977/1.011	2/1.846/1.083
Ba2	2/2.007/0.996	2/2.004/0.998	2/2.009/0.995	2/2.006/0.997	2/2.004/0.998	2/2.020/0.990	2/2.000/1.000	2/2.072/0.965
Ba3	2/2.022/0.989	2/2.001/1.000	2/1.998/1.001	2/2.044/0.979	2/2.024/0.988	2/2.020/0.990	2/2.015/0.993	2/2.154/0.929
M1	3.40/3.423/0.993	3.441/3.462/0.994	3.396/3.419/0.993	3.371/3.373/1.000	3.395/3.402/0.998	3.427/3.495/0.981	3.431/3.452/0.994	3/3.099/0.968
M2	3.40/3.336/1.019	3.260/3.230/1.009	3.230/3.213/1.005	3.190/3.103/1.028	3.140/3.087/1.017	3.130/3.000/1.043	3.120/3.065/1.018	3/2.576/1.165
M3	3.40/3.444/0.987	3.618/3.612/1.002	3.732/3.718/1.004	3.887/3.990/0.974	3.931/3.987/0.986	3.919/3.949/0.992	3.928/3.958/0.992	4/4.352/0.919
Dispersion for cations	0.039	0.017	0.015	0.066	0.038	0.069	0.032	0.271
Cl	−1/−1.007/0.993	−1/−1.007/0.993	−1/−1.007/0.993	−1/−1.007/0.993	−1/−1.007/0.993	−1/−1.007/0.993	−1/−1.007/0.993	−1/−1.007/0.993
O1	−2/−2.000/1.000	−2/−1.973/1.014	−2/−1.967/1.017	−2/−2.032/0.984	−2/−2.012/0.994	−2/−1.945/1.028	−2/−1.990/1.005	−2/−1.838/1.088
O2	−2/−1.974/1.013	−2/−2.003/0.998	−2/−2.008/0.996	−2/−1.949/1.026	−2/−1.972/1.014	−2/−1.985/1.008	−2/−1.985/1.008	−2/−1.988/1.006
O3	−2/−2.147/0.931	−2/−2.141/0.934	−2/−2.127/0.940	−2/−2.118/0.944	−2/−2.093/0.956	−2/−2.423/0.826	−2/−2.153/0.929	−1/−2.032/0.492
Dispersion for anions	0.086	0.083	0.076	0.077	0.057	0.246	0.089	0.603

For each atom, $q/Q/(q/Q)$ is given. The dispersion, σ, measures the deviation of Q with respect to q for the cations and the anions.

systematically gives better results than BV when applied to oxide materials.

Results of the CD calculations for the seven different structures refined in the present paper, and on the previously reported $Ba_5Fe_4PtClO_{13}$ compound [3], are given in Table 5. For these calculations we assumed that platinum in octahedral coordination is Pt(IV). The q/Q ratios for the cations (the maximum deviation from 1 is 0.043 for the preparation labeled 6), as well as the corresponding standard deviation, show that, using the criteria from Nespolo et al. [11], the different structures proposed can be considered as correct. Moreover, the q/Q ratios for the anions are in accordance with a good valence balance for each new structure. This is not the case for the previously reported structure of $Ba_5Fe_4PtClO_{12.5}$ [3] where the q/Q ratio of the O3 atom is 0.492. This value indicates that, contrary to the expected value for this atom (-1, i.e., a half occupied oxygen), the calculated charge is -2.032, which suggests a fully occupied position. Moreover, the strong deviation from 1 (1.165) observed for the $M2$ site of the $Ba_5Fe_4PtClO_{13}$, as well as the large standard deviation (27.71%) calculated for all the cations are the sign of a problem in the structure determination. We believe that the assumption, made by Leib et al. [3] that all the iron is at a valence (III) is false, and at least for three reasons: this CD analysis; in all the preparations we have synthesized with iron and platinum, a mixed valence state is encountered; the presence of Co(IV) is clearly proved in $Ba_5Co_5ClO_{13}$ [2].

4. Conclusion

In all the prepared iron or cobalt oxychlorides containing platinum and isotypic with $Ba_5Co_5ClO_{13}$, Co^{3+} and Co^{4+} or Fe^{3+} and Fe^{4+} are distributed into octahedral and tetrahedral sites, Pt^{4+} also occupying the octahedral sites. With iron, compound without platinum cannot be obtained under the experimental conditions used. With ruthenium, using the same $BaCl_2$ flux, oxychlorides with structures built from the stacking of BaO_3 and double $(BaCl)_2$ were obtained with general formula $Ba_{n+3}M_nCl_2O_{3n+3}$ where n represents the thickness of the octahedral string in the BaO_3 slab. The terms $n = 2$, 3 and 4 have been obtained for $M = $ Ru [15,16] and for mixed occupation of M sites by Ru and another metal ($n = 2$, $Ba_5RuTaO_9Cl_2$ [17] and $Ba_5Ru_{1.6}W_{0.4}O_9Cl_2$ [18], and $n = 3$, $Ba_6Ru_2PtO_{12}Cl_2$ [19] and $Ba_6Ru_{2.5}Mn_{0.5}O_{12}Cl_2$ [20]); finally, the term $n = 5$ has been obtained for $Ba_8Ru_{3.33}Ta_{1.67}O_{18}Cl_2$ [21]. The compounds reported in this paper could represent the term $n = 3$ of a new series $Ba_{n+2}M_nM'_2ClO_{3n+4}$. Synthesis of other terms are in progress and will be reported in forthcoming papers.

References

[1] J. Darriet, M.A. Subramanian, J. Mater. Chem. 5 (4) (1995) 543–552.

[2] K. Yamaura, D.P. Young, T. Siegrist, C. Besnard, C. Svensson, Y. Liu, R.J. Cava, J. Solid State Chem. 158 (2001) 175–179.

[3] W. Leib, H. Mueller-Buschbaum, Z. Anorg. Allg. Chem. 551 (1987) 7–12.

[4] M. Neubacher, H. Mueller-Buschbaum, J. Alloys Comp. 183 (1992) 18–23.

[5] Bruker Analytical X-Ray System, "SAINT+, Version 6.22", Madison, USA, 2001.

[6] G.M. Scheldrick, SADABS, Bruker-Siemens Area Detector Absorption and Other Correction, Version 2.03, Goetingen, Germany, 2001.

[7] V. Petricek, M. Dusek, The Crystallographic Computing System JANA2000, Praha, Czech Republic, 2002.

[8] P.J. Becker, P. Coppens, Acta Crystallogr. A 30 (1974) 148.

[9] L. Katz, R. Ward, Inorg. Chem. 3 (2) (1964) 205–211.

[10] R. Hoppe, S. Voigt, H. Glaum, J. Kissel, H.P. Müller, K. Bernet, J. Less-Common Met. 156 (1989) 105–122.

[11] M. Nespolo, G. Ferraris, H. Ohashi, Acta Crystallogr. B 55 (1999) 902–916.

[12] M. Nespolo, G. Ferraris, G. Ivaldi, R. Hoppe, Acta Crystallogr. B 57 (2001) 652–664.

[13] L. Pauling, J. Am. Chem. Soc. 51 (1929) 1010–1026.

[14] D. Brown, R.D. Shannon, Acta Crystallogr. A 29 (1973) 266–282.

[15] N. Tancret, P. Roussel, F. Abraham, J. Solid State Chem., in press.

[16] J. Wilkens, Hk. Müller-Buschbaum, Acta Chem. Scand. 45 (1991) 812.

[17] J. Wilkens, Hk. Müller-Buschbaum, J. Alloys Comp. 171 (1991) 255.

[18] S.-T. Hong, A.W. Sleight, J. Solid State Chem. 132 (1997) 407.

[19] M. Neubacher, Hk. Müller-Buschbaum, Z. Anorg. Allg. Chem. 609 (1992) 59.

[20] M. Neubacher, Hk. Müller-Buschbaum, Z. Anorg. Allg. Chem. 602 (1991) 143.

[21] J. Wilkens, Hk. Müller-Buschbaum, J. Alloys Comp. 184 (1992) 195.